JPET Fast Forward. Published on December 15, 2005 as DOI: 10.1124/jpet.105.094391

JPET #94391

Cell Death Mechanism and Protective Effect of Erythropoietin after Focal Ischemia in the Whisker-barrel Cortex of Neonatal Rats

Ling Wei, Byung H. Han, Ying Li, Christine L. Keogh, David M. Holtzman and Shan Ping Yu*

Department of Pathology and Laboratory Medicine (L.W., Y.L., C.L.K., S.P.Y.), Department of Pharmaceutical Sciences (S.P.Y.), Medical University of South Carolina, Charleston, SC 29425; Department of Neurology, Molecular Biology & Pharmacology, Hope Center for Neurological Disorders, Washington University, St. Louis, MO 63110 (L.W., B.H.H., D.M.H.); Department of Manufacturing Pharmacy, Seoul National University, Seoul 110-460, South Korea (B.H.H)

Running title: EPO blocks ischemia-induced cell death in the neonatal brain

*. Corresponding author

Shan Ping Yu
Department of Pharmaceutical Sciences
280 Calhoun Street
Medical University of South Carolina
Charleston, SC 29425
Tel. 843-792-2992
Fax. 843-792-1712
E-mail: yusp@musc.edu

Number of text pages: 33
Number of tables: 0
Number of figures: 9
Number of references: 46
Number of words in the Abstract: 250
Number of words in Introduction: 741
Number of words in Discussion: 1154

Abbreviations: CCA, common carotid artery; DEVD-AMC, N-acetyl-Asp-Glu-Val-Asp-7-amino-4-methylcoumarin; EPO, erythropoietin; EPOR, erythropoietin receptor; H&E, hematoxylin and eosin; MCA, middle cerebral artery; P7, postnatal day-7; STAT-5, signal transducers and activators of transcription-5; TTC, triphenyl tetrazolium chloride; TUNEL, terminal deoxynucleotidyl transferase biotin-dUTP nick end labeling.

Abstract

Cell death induced by the combined insult of hypoxia-ischemia in neonatal rodents has been extensively investigated. Ischemia-only-induced cell death, however, has been much less characterized. Based on the notion that 1) ischemic stroke is a relatively common disorder in human neonates, and 2) developing cells are more susceptible to apoptosis, the present study examined whether typical apoptosis was induced by cerebral ischemia in a new neonatal rat model. Erythropoietin (EPO, Epoetin) was tested for its protective effect against ischemia-induced cell death. Postnatal day-7 (P7) rats were subjected to permanent occlusion of the middle cerebral artery (MCA) branch supplying the right whisker-barrel cortex. TUNEL positive cells in the ischemic region were detectable 4 hrs after ischemia and reached a peak level 16 hrs later. The cell death was preceded by caspase activation and cytochrome c release. Cell body shrinkage was evident among damaged cells. Agarose gel electrophoresis showed DNA damage with a smear pattern as well as DNA laddering. Electron microscopy demonstrated apoptotic features such as cell shrinkage, chromatin condensation and fragmentation; meanwhile, necrotic alterations coexisted in the cytoplasm. EPO treatment increased STAT-5 and Bcl-2 levels, markedly attenuated apoptotic cell death and reduced ischemic infarct in the cortex. It is suggested that focal ischemia in the developing brain causes cell death with prominent apoptotic features coexisting with some characteristics of necrosis. This is consistent with the concept of hybrid death previously described in cultures and adult or developing brain. EPO may be explored as a potential therapy for neonatal ischemic stroke.

Introduction

Ischemic stroke affects not only elderly but also young individuals. Recent studies have recognized that arterial ischemic stroke in infants and children is an important cause of morbidity and mortality and an emerging area for clinical and translational research (Lynch et al., 2002; Lee et al., 2005). The few days before and after birth are high risk periods for stroke for both the mother and the infant. This is probably related to activation of coagulation mechanisms in this critical period. Perinatal arterial ischemic stroke is recognized in about one in 4,000 full-term infants, which is higher than previously recognized (Nelson and Lynch, 2004). Specifically, neonatal stroke involving middle cerebral artery (MCA) occlusion may occur in term infants (Govaert et al., 2000; Ashwal and Pearce, 2001) and more than 80% of neonatal strokes involve the vascular territory supplied by the MCA (Ashwal and Pearce, 2001). Among ischemic stroke, focal cerebral ischemia may account for more cases of brain lesions in preterm and full term neonates and may be more prevalent than global cerebral ischemia due to systemic asphyxia. Compared with investigations on adult ischemic stroke, much less attention has been paid to understanding the mechanism and treatment of perinatal, neonatal, and childhood strokes (Lynch et al., 2002).

Apoptosis has been identified as a typical mechanism of cell death in the developing brain. Features of apoptosis are prominent in the neonatal brain subjected to a hypoxia-ischemia insult (Cheng et al., 1998; Nakajima et al., 2000). Apoptosis was also observed following transient focal ischemia in neonatal rats (Renolleau et al., 1998; Manabat et al., 2003). However, some reports suggest that the neuronal cell death induced by hypoxia-ischemia in neonates is not apoptosis (van Lookeren Campagne and

Gill, 1996). A study on neonatal mouse hippocampus showed that even delayed cell death after hypoxia-ischemia does not have classic features of apoptosis (Sheldon et al., 2001). Whether or not typical apoptosis takes place after permanent cerebral ischemia in neonates remains elusive.

The ischemia-induced neonatal brain damage induced by transient or permanent cerebral ischemia has been studied in postnatal day-7 (P7) rat pups (Renolleau et al., 1998; Manabat et al., 2003; Wen et al., 2004). The MCA suture ligation used in these models successfully induces cell death in ischemic and penumbra regions and causes infarct in the ipsilateral hemisphere including cortical and subcortical regions. Small strokes, on the other hand, often occur in clinical settings. To date, however, there has been no animal model in which small strokes are induced in the neonatal brain. Based on our previous "mini-stroke" model of whisker-barrel cortex in adult rats (Wei et al., 1995; Wei et al., 2001), we now report a new ischemic model of whisker-barrel cortex stroke in neonatal rats.

The hematopoietic factor erythropoietin (EPO, Epoetin) has been proposed as a potent neuroprotective drug in the treatment of ischemic stroke (Sakanaka et al., 1998; Bernaudin et al., 1999). Numerous studies have shown that EPO function is not limited to the hematopoietic system; EPO and functional EPO receptor (EPOR) have been identified in a wide variety of cells in rodents, primates and humans (Digicaylioglu et al., 1995; Marti, 2004). EPO and EPOR are highly expressed in the developing brain, suggesting that they play important roles in neural development (Dame et al., 2000; Juul, 2002). A hypoxic-ischemic insult increased the expression of endogenous EPO and EPOR in the neonatal rat brain (Spandou et al., 2004), and permanent focal cerebral

ischemia activated EPOR in the neonatal rat brain (Wen et al., 2004). EPO is neuroprotective against apoptosis induced by ischemic insults *in vivo* (Bernaudin et al., 1999; Digicaylioglu and Lipton, 2001; Wen et al., 2002) and against hypoxic-ischemic brain injury in neonatal rats (Kumral et al., 2003; Demers et al., 2005). It also improves functional and histological outcome in neonatal stroke in P10 rats (Chang et al., 2005). Using the ischemic model of whisker-barrel cortex stroke, the present study investigated the cell death mechanism induced by a pure ischemic insult in neonatal rats and explored the potential neuroprotective effect of EPO against the ischemia-induced cell death. The effects of EPO treatment on the EPOR-JAK-2 downstream target signal transducers and activators of transcription-5 (STAT-5) and the anti-apoptotic gene Bcl-2 were explored.

Materials and Methods

Whisker-barrel cortex ischemic stroke in neonatal rats

Wistar rats of P7 of both sexes were anesthetized by 3% isoflurane in a mixture of 70% N_2O and 30% O_2. Following induction of anesthesia, 1.5% isoflurane was maintained with mechanical ventilation. Body temperature was monitored and maintained at 36 - 37 °C with a combination of overhead lights and a heating blanket. Surgical procedures to induce barrel cortex ischemia in adult rats have previously been reported (Wei et al., 1995; Wei et al., 2001), barrel cortex ischemia in this investigation was induced similarly with modifications for neonates. Animals were placed in a noninvasive head holder and a 2.5 - 3.0-mm diameter craniectomy was performed through the right parietal skull and the transparent dura was left intact over the whisker barrel cortex. Under a dissecting microscope, sterile #11 silk sutures were passed through the dura to ligate a proximal branch of MCA. To ensure sufficient reduction in the blood supply, the common carotid artery (CCA) was additionally occluded for 10 min. Most likely because of the less developed collateral circulation in the neonate, this ligation method was sufficient to induce a selective damage in the barrel cortex (see Fig. 1). In sham controls, ligatures were placed through the dura and under arterial branches and CCA but not tied. After surgery and waking up, the pups were returned to their mothers for recovery. Recombinant EPO (Amgen, Inc., Thousand Oaks, CA) was i.p. injected according to the experimental plan.

Ischemic infarct volume assay

Post surgery rats were subsequently sacrificed at various times after ischemia. Animals were killed with an overdose of pentobarbital (100 mg/kg) followed by

intracardiac perfusion with 200 ml of 0.9% NaCl. Brains were then sliced into 2-mm coronal sections using a rat brain matrice (Harvard Bioscience, South Natick, MA). The cortical infarct volume was morphometrically measured after triphenyl tetrazolium chloride (TTC) stain. The brain slices were incubated in phosphate-buffered saline (pH 7.4) containing 2% TTC at 37 ^{o}C for 20 min and then stored in 10% neutral-buffered formalin. A cross-sectional area of the TTC-unstained region for each brain slice was determined using an image analyzer (MCID Imaging System, Imaging Research Inc., St. Catharines, Ontario, Canada) and the indirect method (subtraction of residual right hemisphere cortical volume from the cortical volume of the intact left hemisphere). Hemisphere cortical volume was calculated by summation of infarct volumes measured in component brain slices. Infarct assessments were performed under blind condition.

Hematoxylin and eosin (H&E) analysis

After sacrifice, animals were perfused with 4% paraformaldehyde and brain 8-µm sections were prepared for H&E staining following standard histochemical procedures (Luna, 1968).

Terminal deoxynucleotidyl transferase biotin-dUTP nick end labeling (TUNEL)

Animals under anesthesia underwent perfusion fixation with 200 ml of normal saline followed by 10% formalin at different hours after ischemia. Parafin-embedded brain sections of 10 µm were deparaffinized in two changes of xylene for 5 min each, then washed sequentially in 100, 95, and 70% ethanol. Nuclei of tissue sections were stripped of proteins by incubation with 20 µg/ml proteinase K (Sigma, St. Louis, MO) for 5 min. Slices were washed in distilled water. The new 3'-OH DNA ends generated by DNA fragmentation typically localized in nuclei were stained using the ApopTAg in situ

apoptosis detection kit (S7110-Kit, Oncor. Inc., Gaithersburg, MD). For double staining with Hoechst, brain sections were then incubated with 10 µM Hoechst 33285 for 2 min.

Caspase-3 activation of immunohistochemical staining

Activated caspase-3 was visualized by CM1 antibody or caspase-3 immunoassay/activity kit (Calbiochem, San Diego, CA). The rabbit polyclonal antiserum CM1 recognizes the p18 subunit of cleaved caspase 3 and has been used as a specific detector for caspase-3 activation. Frozen brain sections of 10-µm thick were fixed and then incubated with 2% Triton X-100 for 30 min followed by PBS wash. Brain sections were processed for peroxidase immunohistochemistry using the CM1 antibody (1:20,000) with the Vectastain ABC Elite kit (Vector Laboratories, Burlingame, CA) or incubated with anti-caspase-3 antibody (1:100; 1 hr), rinsed in PBS 3 times. For NeuN double labeling, additional incubation with the NeuN antibody (1:200; 2 hrs) was performed. After wash, sections were counterstained with bisbenzimide (5 min and rinse) and coversliped in Vectashield. Cell staining was visualized under a Nikon fluorescent microscope (Nikon TE-2000, NikonUSA, Melville, NY) and photographed.

Caspase catalytic activity was also measured as previously described (Han and Holtzman, 2000). Briefly, tissue homgenates were lysed in 80 µl of buffer A (10 mM HEPES, 42 mM KCl, 5 mM $MgCl_2$, 1 mM DTT, 1% Triton X-100, 1 mM PMSF, 1 µg/mL leupeptin, pH 7.4). Lysate (10 µl) was combined in a 96-well plate with 90 µl of buffer B (10 mM HEPES, 42 mM KCl, 5 mM $MgCl_2$, 1 mM DTT, 1% Triton X-100, 10% sucrose, pH 7.4) containing fluorometric substrate (30 µM) and incubated for 45 min at room temperature in the dark. Formation of fluorogenic product was determined in a cytofluor fluorometric plate reader by measuring emission at 460 nm with 360 nm

excitation. Caspase-3 like activity was correlated with cleavage of N-acetyl-Asp-Glu-Val-Asp-7-amino-4-methylcoumarin (DEVD-AMC).

Cytochrome c immunohistochemistry

Anesthetized animals were perfused with 10 U/ml heparin and subsequently with 4% formaldehyde in 0.1 M PBS, pH 7.4. The brains were removed, post-fixed for 12 hrs, sectioned at 25 µm on a vibratome, and processed for immunohistochemistry. The sections were incubated with a blocking solution and reacted with rabbit anti-cytochrome c polyclonal antibody (Santa Cruz Biotechnology, Santa Cruz, CA) at a dilution of 1:200. Primary antibody binding was detected by incubating the sections with the Vectastain ABC Elite kit (Vector Laboratories, Santa Cruz, CA). As a negative control, sections were incubated without primary antibodies.

Determination of DNA fragmentation **(laddering)**

Homogenates of the ipsilateral cortex (ischemic and penumbra regions) were obtained from the sham-operated and ischemic stroke animals; resuspended in lysis buffer (10 mM Tris-HCl, 100 mM EDTA, 0.5 % SDS; pH 8.0) for 5 min at room temperature and then treated with Proteinase K (300µg/ml) for 2 hrs at 50 ^{o}C. DNA was precipitated overnight at 4 ^{o}C by adding NaCl to a final concentration of 1 M. The lysate was centrifuged at 13,000 rpm for 1 hr at 4 ^{o}C followed by extraction of DNA with phenol/chloroform/isoamyl alcohol (25:24:1). The total DNA contained in the aqueous phase was precipitated with isopropanol. The DNA pellet was washed twice with 70% ethanol and resuspended in TE buffer containing RNase at 0.3 mg/ml. Aliquots (10 - 15 µg of DNA) were analyzed on a 1.5% agarose gel and run at 75 V for 3 hrs. Following

electrophoresis and staining with ethidium bromide the gel was visualized under ultraviolet light and photographed.

Cell surface area and cell death assessments

Cell surface area was assessed using the imaging analysis software ANALYSIS (Soft Imaging System Cop., Lakewood, CO) on 10 randomly chosen non-overlapping fields of 3 cortical areas of the ipsilateral and contralateral hemispheres under 40x magnification.

Cell death in the ischemic areas of coronal brain sections was evaluated by counting TUNEL and activated caspase-3 positive cells and their ratios to the total cells counterstained with Hoechst 33285 or Propidium Iodide. Ten nonoverlapping microscopic fields of 3 cortical areas of the ipsilateral hemisphere were counted in 1.25 mm^2 areas in the ischemic region under 40x magnification. A stereological count of total cells and double-labeled cells were conducted on every 10^{th} section so cell counting was performed on slices 90 μm apart to avoid repeated counting of the same cells. Cell counts were confirmed by additional counting on confocal images. Average numbers and ratios of a cell type to total cells per field were calculated. Cell surface assay and cell counting were performed under blind condition.

Western blotting of STAT-5 and Bcl-2

Tissue samples were taken from the ipsilateral cortex with and without EPO treatment. Proteins were extracted using the NE-PER Nuclear and Cytoplasmic Extraction Kit (Pierce Biotechnology, Rockford, IL). Protein concentration of each sample was determined using the Bicinchoninic Acid Assay (Sigma, St. Louis, MO). Proteins from each sample (50 μg) were separated by SDS-PAGE in a Hoefer Mini-Gel

system (Amersham Biosciences, Piscataway, NJ) and transferred in the Hoefer Transfer Tank (Amersham Biosciences, Piscataway, NJ) to a PVDF membrane (BioRad, Hercules, CA). Membranes were blocked in 7% evaporated milk diluted in Tris-buffered saline containing 0.1% Tween-20 (TBS-T) at room temperature for at least 2 hours, and then incubated with polyclonal rabbit anti-phospho-STAT-5 (Santa Cruz Biotechnology, Santa Cruz, CA) or polyclonal rabbit anti-Bcl-2 antibody (Oncogene Science, Cambridge, MA). A mouse β-actin antibody (Sigma, St. Louis, MO) was used for protein loading control. After primary antibody incubation, membranes were washed with TBS-T and incubated with alkaline phosphatase-conjugated anti-rabbit IgG (Promega, Madison, WI) antibody for 2 hours at room temperature. Finally, membranes were washed with TBS-T followed by three washes with TBS and signal was detected by the addition of BCIP/NBT solution (Sigma, St. Louis, MO).

Electron microscopy

For ultrastructural examination, sacrificed rats were perfused intra-aortically with glutaraldehyde 2% in 0.1 M phosphate buffer. After perfusion, the brains were removed and postfixed for 1 day in the same solution. Ultrathin sections through dentate gyrus and cerebral cortex were cut on a Reichert Ultracut Ultramicrotome (Mager Scientific Inc., Dexter, MI), mounted on 150-mesh copper grids, and poststained in uranyl acetate and Reynold's lead citrate. Sections were photographed using a transmission electronic microscope (Zeiss 902, Carl Zeiss, Inc, Thornwood, NY) (Wei et al., 2004).

Statistics

Student's two-tailed t test was used for comparison of two experimental groups. In the event that there was a doubt that samples might not come from normally distributed populations, Rank Sum Tests were performed using SigmaStat (SYSTAT Software, Inc., Point Richmond, CA). Multiple comparisons were analyzed using one-way ANOVA followed by a post-hoc Tukey test for multiple pairwise examinations. Changes were identified as significant if *P* was less than 0.05. Mean values were reported together with the standard deviation.

Results

Focal ischemic stroke in the neonatal barrel cortex

In the P7 newborn rat, permanent occlusion of the MCA branch supplying the whisker-barrel cortex caused a visible ipsilateral cortical infarct 12 hrs after the insult (Fig. 1). H&E staining showed significant cell damage in the ischemic region 6 hrs after the ischemic insult; injured cells appeared dark and showed shrunken cell bodies with condensed nuclei (Fig. 1). In the ischemic region, the apoptotic feature of cell shrinkage was evident; the cell surface area became much smaller than that in the contralateral side of the brain (Fig. 2), which was a sign of apoptotic injury.

Cell death was further identified using TUNEL staining. Noticeable TUNEL positive cells were seen in the ischemic region 4 hrs after initiation of ischemia and reached a peak level 24 hrs after the insult (Fig. 3A and 3B). The TUNEL positive cells had shrunken cell bodies and condensed nuclei. Specifically, nuclear fragmentation was seen in many TUNEL positive cells (type II TUNEL positive cells) (Wei et al., 2004), which indicated an apoptotic nature or an apoptotic component of the injury (Fig. 3A). Conversely, only a few TUNEL positive cells were detected in the normal or contralateral side of the brain (data not shown).

Ischemia-induced hybrid cell death of apoptotic and necrotic changes in neonatal brain

To confirm the apoptotic nature of the cell death, caspase-3 activation in the ischemic brain was visualized with the anti-CM-1 antibody or the anti-caspase-3 polyclonal antibody, which recognizes the activated form of caspase-3 (Fig. 4A and 4B).

To quantify the catalytic activity of activated caspase-3, we also measured the cleavage of N-acetyl-Asp-Glu-Val-Asp-7-amino-4-methylcoumarin (DEVD-AMC). Evidence of caspase-3 activation was seen in the ipsilateral but not the contralateral cortex. Activation reached a plateau level about 8 hrs after ischemia and persisted for about one day before gradually declining towards the normal level (Fig. 4C). The ischemia-induced cell death was also characterized by cytochrome c release. Using immunohistochemical staining, cytochrome c in the cytoplasm was detected 6-12 hrs after ischemia (Fig. 5).

Apoptosis is characterized by DNA laddering of ~180 base pair breaks detectible on an agarose gel by electrophoresis. During the first few hours after ischemia, DNA isolated from the ipsilateral cortex in the region of the ischemia showed predominantly a smear on agarose gels, suggesting a necrotic injury. From 8 hrs post-ischemia, DNA laddering became visible in the ipsilateral brain. Apoptotic-like DNA fragmentation was more evident 16 hrs after ischemia (Fig. 6).

To confirm morphological features of cell death and to verify whether necrotic and apoptotic alterations evolved in parallel with each other or in sequence, electron microscopy was performed 8, 16 and 24 hrs after the onset of ischemic insult. Damaged neurons showed marked cytoplasm shrinkage, nuclear/chromatin condensation and a large amount of fragmentation, consistent with apoptotic morphology (Fig. 7). In later stages, apoptotic bodies of intact membrane containing condensed dark chromatin masses formed in many cells; some apoptotic bodies even fell off the cells (Fig. 7). On the other hand, it was also evident that, at all time points examined, most cells showed vacuolated cytoplasm coexisting with condensed nuclei and/or apoptotic body

formation. The deteriorating cytosol and disrupted membranes indicated a necrotic component throughout the time period after ischemia. Thus concurrent morphological features of both apoptosis and necrosis, or hybrid cell death, took place after the cerebral ischemia (Fig. 7).

Neuroprotection of EPO against ischemia-induced cell death and infarct formation in the neonatal brain

Systemic administration of recombinant EPO (10,000 U/kg, i.p.) was given to animals 5-10 min before MCA occlusion and repeated once a day after ischemia. No gross adverse effects of EPO were observed. The EPO treatment significantly reduced caspase-3 activation (Fig. 8B and 8C) and the percentage of TUNEL positive cells (Fig. 8B and 8D). Consistently, EPO showed a remarkable protective action of reducing ischemic infarct volume (Fig. 8A, 8E and 8F). Suggesting a lasting EPO protection, the brain weight of EPO-treated rats measured 5 weeks after ischemia was significantly greater than that of time matched saline control rats (1.67 ± 0.02 g vs. 1.54 ± 0.02 g, n = 7 and 6, respectively, $P < 0.05$; EPO 10,000 U/kg, i.p. before ischemia and once a day for 10 days after ischemia).

EPO induced increases of STAT-5 and Bcl-2 expression in the ischemic brain

To understand the possible mechanism mediating the EPO neuroprotection, we examined the level of phosphorylated STAT-5, a downstream signal of the EPO-JAK-2 pathway. Examined at 12 and 24 hrs after ischemia, animals that received EPO injection (10,000 U/kg, i.p. before ischemia) showed increased level of STAT-5 in the ipsilateral

cortex compared with that of ischemia-only animals (Fig. 9A). EPO treatment also enhanced expression of the anti-apoptotic gene Bcl-2 in the ipsilateral cortex (Fig. 9B).

Discussion

Although extensive investigations have studied neonatal brain damage induced by combined insults of hypoxia plus ischemia, neonatal stroke induced by ischemia alone has been much less studied. The nature of neonatal cell death after an ischemia insult remains obscure. The present investigation examined the neuronal death solely induced by permanent ligation of the MCA branch supplying to the cerebral sensorimotor cortex of neonatal rats. Marked apoptotic alterations are identified as a primary feature of neuronal cell death in this ischemia model. Apoptosis was demonstrated as shrunken cells that were positive for TUNEL and caspase-3 staining, cytochrome c release, DNA laddering, and characteristic ultrastructural changes. Meanwhile, a noticeable necrotic component was revealed by DNA smearing, vacuolated cytoplasm, and collapsed membranes at subcellular and ultrastructural levels. These observations correspond with a previous study of hypoxia-ischemia-induced hybrid cell death in the newborn rat (Nakajima et al., 2000). EPO, as shown in various other animal model studies, exhibited significant neuroprotection against ischemic infarct formation and cell death in the neonatal brain. The result is consistent with a very recent report showing that after focal cerebral ischemia, EPO activates several pathways and attenuates brain injury in P7 rats (Sola et al., 2005).

Neonatal stroke animal models are essential for understanding the mechanism of cell death and exploring potential therapeutic treatments in neonatal stroke. The most commonly used rodent model of neonatal stroke is the combined insult of hypoxia-ischemia in rats at postnatal day 7. This model is performed by ligation of unilateral carotid artery and exposure to systemic hypoxia for 2-3 hrs, which results in a

reproducible unilateral brain damage ipsilateral to the ligated artery. Many pathophysiological mechanisms related to hypoxia-ischemia have been studied using these models (Yager and Thornhill, 1997; Cheng et al., 1998; Ashwal and Pearce, 2001). The P7 rats are used based on the notion that the developmental stage of these pups corresponds to that of a near term human (McIlwain, 1971). The hypoxia-ischemia model, however, requires the application of systemic hypoxia that may not imitate the pathophysiological condition of pure focal ischemia. Ligation of extracranial vessels with superimposed hypoxia in this model is also different from obstruction of cerebral blood flow of focal stroke in human neonates. To understand the ischemia-induced injury in the developing brain, ischemic stroke neonatal animal models have been used in some previous investigations (Renolleau et al., 1998; Manabat et al., 2003; Wen et al., 2004). The neonatal model in the present study was developed based on our previous barrel stroke model in adult rats (Wei et al., 1995; Wei et al., 2001). The MCA branch occlusion used in the present investigation provides an ischemic stroke model of neonates that mimics small strokes often observed in clinical cases.

The developing brain is different from the mature brain in a number of structural and functional characteristics (Johnston et al., 2002; Herlenius and Lagercrantz, 2004). During development, brain susceptibility to hypoxia and ischemia varies greatly (Muramatsu et al., 1997; Yager and Thornhill, 1997). Compared with the adult brain, the neonatal brain shows higher tolerance to hypoxic and ischemic insults (Singer, 1999; Johnston et al., 2002); on the other hand, neurons in the neonatal brain are more susceptible to die from apoptosis (Dikranian et al., 2001; Johnston et al., 2002). The development of typical necrotic and apoptotic cell death by distinct insults has been

explicitly demonstrated in *in vitro* studies. The nature of ischemic cell death *in vivo*, however, has not been well defined. Increasing evidence indicates that, except for severe attacks such as cell death in the ischemic core region of adult animals, a mixed form of necrosis and apoptosis appears as a common pathological occurrence (Eichenbaum et al., 2002; Liu et al., 2004; Wei et al., 2004). Our previous studies showed concurrent apoptotic and necrotic alterations in the same cells after different insults such as energy deficiency, reactive oxygen induction *in vitro*, and focal ischemia in adult animals (Xiao et al., 2002; Wei et al., 2004). During normal development, classical apoptosis occurs in the neonatal brain. In the setting of neonatal brain injury, cells can die with many features of apoptosis although there are morphological differences between natural cell death during development vs. in the setting of injury. The present study largely supports the idea that cell death with apoptotic features is a primary form of neuronal injury induced by focal ischemia in the neonatal brain. However, even in the neonatal brain, a necrotic component coexists in the same cells as those with apoptotic features. We agree with the notion that detection of an apoptotic process such as caspase activation and/or DNA laddering does not conclude typical apoptotic cell death. On the other hand, some coexisting necrotic alterations should not renounce apoptosis in the death mechanism. The characteristics of hybrid cell death imply that therapies that target both apoptosis and necrosis are necessary to protect neurons against ischemic insults in adults as well as in neonates.

As a downstream signal of HIF-1α, EPO increases after ischemic or hypoxic insults (Bernaudin et al., 1999; Digicaylioglu and Lipton, 2001; Marti, 2004). Recent studies in neonatal rats showed a significant increase in EPO receptor protein in the

ischemic areas 6-12 hrs after permanent focal cerebral ischemia (Wen et al., 2004). Endogenous EPO has also been shown to increase in the ipsilateral cortex 1-7 days after hypoxia-ischemia (Spandou et al., 2004; Sun et al., 2004). EPO showed marked neuroprotection against brain injury, especially apoptosis, after neonatal hypoxia-ischemia, partially mediated by the activation of HSP27 (Kumral et al., 2003; Sun et al., 2004). EPO increases the expression of the anti-apoptotic gene Bcl-X_L and decreases the expression of the pro-apoptotic gene Bak in PC12 cells (Renzi et al., 2002). EPO may regulate the balance of the Bcl/Bax ratio towards a net anti-apoptotic effect in cultured microglia and neurons (Vairano et al., 2002; Wen et al., 2002). Subsequently, EPO inhibits caspase activities linked to cytochrome *c* release (Chong et al., 2003).

Although the JAK-2-STAT-5 pathway is well established as a downstream signal of EPO receptor activation, its role in EPO-induced neuroprotection in the ischemic brain remains poorly defined. Our study provides new evidence that EPO treatment *in vivo* activates STAT-5 signaling. We showed that EPO enhanced the phosphorylated STAT-5, which could not only in turn increase anti-apoptotic gene Bcl-X_L (Wen et al., 2002; Sola et al., 2005), but also increase another major anti-apoptotic gene Bcl-2. The EPO-increased anti-apoptotic genes and its inhibitory effect on caspase activation afford a prominent anti-apoptotic action. Since EPO has been shown to be protective against both apoptosis and necrosis (Joyeux-Faure et al., 2005), the present study strongly supports the possibility that EPO and its analogues may be explored as therapeutic drugs for the treatment of neonatal stroke.

References

Ashwal S and Pearce WJ (2001) Animal models of neonatal stroke. *Curr Opin Pediatr* **13**:506-516.

Bernaudin M, Marti HH, Roussel S, Divoux D, Nouvelot A, MacKenzie ET and Petit E (1999) A potential role for erythropoietin in focal permanent cerebral ischemia in mice. *J Cereb Blood Flow Metab* **19**:643-651.

Chang YS, Mu D, Wendland M, Sheldon RA, Vexler ZS, McQuillen PS and Ferriero DM (2005) Erythropoietin improves functional and histological outcome in neonatal stroke. *Pediatr Res* **58**:106-111.

Cheng Y, Deshmukh M, D'Costa A, Demaro JA, Gidday JM, Shah A, Sun Y, Jacquin MF, Johnson EM and Holtzman DM (1998) Caspase inhibitor affords neuroprotection with delayed administration in a rat model of neonatal hypoxic-ischemic brain injury. *J Clin Invest* **101**:1992-1999.

Chong ZZ, Kang JQ and Maiese K (2002) Hematopoietic factor erythropoietin fosters neuroprotection through novel signal transduction cascades. *J Cereb Blood Flow Metab* **22**:503-514.

Chong ZZ, Kang JQ and Maiese K (2003) Apaf-1, Bcl-xL, cytochrome c, and caspase-9 form the critical elements for cerebral vascular protection by erythropoietin. *J Cereb Blood Flow Metab* **23**:320-330.

Dame C, Bartmann P, Wolber E, Fahnenstich H, Hofmann D and Fandrey J (2000) Erythropoietin gene expression in different areas of the developing human central nervous system. *Brain Res Dev Brain Res* **125**:69-74.

Demers EJ, McPherson RJ and Juul SE (2005) Erythropoietin protects dopaminergic neurons and improves neurobehavioral outcomes in juvenile rats after neonatal hypoxia-ischemia. *Pediatr Res* **58**:297-301.

Digicaylioglu M, Bichet S, Marti HH, Wenger RH, Rivas LA, Bauer C and Gassmann M (1995) Localization of specific erythropoietin binding sites in defined areas of the mouse brain. *Proc Natl Acad Sci U S A* **92**:3717-3720.

Digicaylioglu M and Lipton SA (2001) Erythropoietin-mediated neuroprotection involves cross-talk between Jak2 and NF-kappaB signalling cascades. *Nature* **412**:641-647.

Dikranian K, Ishimaru MJ, Tenkova T, Labruyere J, Qin YQ, Ikonomidou C and Olney JW (2001) Apoptosis in the in vivo mammalian forebrain. *Neurobiol Dis* **8**:359-379.

Eichenbaum JW, Pevsner PH, Pivawer G, Kleinman GM, Chiriboga L, Stern A, Rosenbach A, Iannuzzi K and Miller DC (2002) A murine photochemical stroke model with histologic correlates of apoptotic and nonapoptotic mechanisms. *J Pharmacol Toxicol Methods* **47**:67-71.

Govaert P, Matthys E, Zecic A, Roelens F, Oostra A and Vanzieleghem B (2000) Perinatal cortical infarction within middle cerebral artery trunks. *Arch Dis Child Fetal Neonatal Ed* **82**:F59-63.

Han BH and Holtzman DM (2000) BDNF protects the neonatal brain from hypoxic-ischemic injury in vivo via the ERK pathway. *J Neurosci* **20**:5775-5781.

Herlenius E and Lagercrantz H (2004) Development of neurotransmitter systems during critical periods. *Exp Neurol* **190 Suppl 1**:S8-21.

Johnston MV, Nakajima W and Hagberg H (2002) Mechanisms of hypoxic neurodegeneration in the developing brain. *Neuroscientist* **8**:212-220.

Joyeux-Faure M, Godin-Ribuot D and Ribuot C (2005) Erythropoietin and myocardial protection: what's new? *Fundam Clin Pharmacol* **19**:439-446.

Juul SE (2002) Erythropoietin in the central nervous system, and its use to prevent hypoxic-ischemic brain damage. *Acta Paediatr Suppl* **91**:36-42.

Kumral A, Ozer E, Yilmaz O, Akhisaroglu M, Gokmen N, Duman N, Ulukus C, Genc S and Ozkan H (2003) Neuroprotective effect of erythropoietin on hypoxic-ischemic brain injury in neonatal rats. *Biol Neonate* **83**:224-228.

Lee J, Croen LA, Backstrand KH, Yoshida CK, Henning LH, Lindan C, Ferriero DM, Fullerton HJ, Barkovich AJ and Wu YW (2005) Maternal and infant characteristics associated with perinatal arterial stroke in the infant. *Jama* **293**:723-729.

Liu CL, Siesjo BK and Hu BR (2004) Pathogenesis of hippocampal neuronal death after hypoxia-ischemia changes during brain development. *Neuroscience* **127**:113-123.

Luna LG (1968) *Manual of histologic staining methods of the armed forces institute of pathology*. McGraw-Hill, New York.

Lynch JK, Hirtz DG, DeVeber G and Nelson KB (2002) Report of the National Institute of Neurological Disorders and Stroke workshop on perinatal and childhood stroke. *Pediatrics* **109**:116-123.

Manabat C, Han BH, Wendland M, Derugin N, Fox CK, Choi J, Holtzman DM, Ferriero DM and Vexler ZS (2003) Reperfusion differentially induces caspase-3 activation in ischemic core and penumbra after stroke in immature brain. *Stroke* **34**:207-213.

Marti HH (2004) Erythropoietin and the hypoxic brain. *J Exp Biol* **207**:3233-3242.

McIlwain H, Bachelard,H.S. (1971) Chemical and enzymatic makeup of the brain during development and ageing., in *Biochemistry and the central nervous system* (Wilkins W ed) pp 371-412, The Williams and Wikins Company, Baltimore, MD.

Muramatsu K, Fukuda A, Togari H, Wada Y and Nishino H (1997) Vulnerability to cerebral hypoxic-ischemic insult in neonatal but not in adult rats is in parallel with disruption of the blood-brain barrier. *Stroke* **28**:2281-2288; discussion 2288-2289.

Nakajima W, Ishida A, Lange MS, Gabrielson KL, Wilson MA, Martin LJ, Blue ME and Johnston MV (2000) Apoptosis has a prolonged role in the neurodegeneration after hypoxic ischemia in the newborn rat. *J Neurosci* **20**:7994-8004.

Nelson KB and Lynch JK (2004) Stroke in newborn infants. *Lancet Neurol* **3**:150-158.

Renolleau S, Aggoun-Zouaoui D, Ben-Ari Y and Charriaut-Marlangue C (1998) A model of transient unilateral focal ischemia with reperfusion in the P7 neonatal rat: morphological changes indicative of apoptosis. *Stroke* **29**:1454-1460.

Renzi MJ, Farrell FX, Bittner A, Galindo JE, Morton M, Trinh H and Jolliffe LK (2002) Erythropoietin induces changes in gene expression in PC-12 cells. *Brain Res Mol Brain Res* **104**:86-95.

Sakanaka M, Wen TC, Matsuda S, Masuda S, Morishita E, Nagao M and Sasaki R (1998) In vivo evidence that erythropoietin protects neurons from ischemic damage. *Proc Natl Acad Sci U S A* **95**:4635-4640.

Sheldon RA, Hall JJ, Noble LJ and Ferriero DM (2001) Delayed cell death in neonatal mouse hippocampus from hypoxia-ischemia is neither apoptotic nor necrotic. *Neurosci Lett* **304**:165-168.

Singer D (1999) Neonatal tolerance to hypoxia: a comparative-physiological approach. *Comp Biochem Physiol A Mol Integr Physiol* **123**:221-234.

Sola A, Rogido M, Lee BH, Genetta T and Wen TC (2005) Erythropoietin after focal cerebral ischemia activates the Janus kinase-signal transducer and activator of transcription signaling pathway and improves brain injury in postnatal day 7 rats. *Pediatr Res* **57**:481-487.

Spandou E, Papoutsopoulou S, Soubasi V, Karkavelas G, Simeonidou C, Kremenopoulos G and Guiba-Tziampiri O (2004) Hypoxia-ischemia affects erythropoietin and erythropoietin receptor expression pattern in the neonatal rat brain. *Brain Res* **1021**:167-172.

Sun Y, Zhou C, Polk P, Nanda A and Zhang JH (2004) Mechanisms of erythropoietin-induced brain protection in neonatal hypoxia-ischemia rat model. *J Cereb Blood Flow Metab* **24**:259-270.

Vairano M, Dello Russo C, Pozzoli G, Battaglia A, Scambia G, Tringali G, Aloe-Spiriti MA, Preziosi P and Navarra P (2002) Erythropoietin exerts anti-apoptotic effects on rat microglial cells in vitro. *Eur J Neurosci* **16**:584-592.

van Lookeren Campagne M and Gill R (1996) Ultrastructural morphological changes are not characteristic of apoptotic cell death following focal cerebral ischaemia in the rat. *Neurosci Lett* **213**:111-114.

Wei L, Erinjeri JP, Rovainen CM and Woolsey TA (2001) Collateral growth and angiogenesis around cortical stroke. *Stroke* **32**:2179-2184.

Wei L, Rovainen CM and Woolsey TA (1995) Ministrokes in rat barrel cortex. *Stroke* **26**:1459-1462.

Wei L, Ying DJ, Cui L, Langsdorf J and Yu SP (2004) Necrosis, apoptosis and hybrid death in the cortex and thalamus after barrel cortex ischemia in rats. *Brain Res* **1022**:54-61.

Wen TC, Rogido M, Genetta T and Sola A (2004) Permanent focal cerebral ischemia activates erythropoietin receptor in the neonatal rat brain. *Neurosci Lett* **355**:165-168.

Wen TC, Sadamoto Y, Tanaka J, Zhu PX, Nakata K, Ma YJ, Hata R and Sakanaka M (2002) Erythropoietin protects neurons against chemical hypoxia and cerebral ischemic injury by up-regulating Bcl-xL expression. *J Neurosci Res* **67**:795-803.

Xiao AY, Wei L, Xia S, Rothman S and Yu SP (2002) Ionic mechanism of ouabain-induced concurrent apoptosis and necrosis in individual cultured cortical neurons. *J Neurosci* **22**:1350-1362.

Yager JY and Thornhill JA (1997) The effect of age on susceptibility to hypoxic-ischemic brain damage. *Neurosci Biobehav Rev* **21**:167-174.

Footnotes

Supported by NIH NS35902 (DMH), NS37337, NS42236, NS045155, NS045810, and American Heart Association and Bugher Foundation (AHA-Bugher) Awards 0170064N and 0170063N.

Figure Legends

Figure 1. Focal ischemia induced infarct in the neonatal brain

Focal ischemia-induced cell damage in the ischemic barrel cortex. **A** to **D**. H&E staining in a 10-μm brain section shows normal neurons (arrow head in A) and cellular damage (arrows in B to D) at different time points after ischemia. Significant cell body shrinkage and condensation of dark nuclei were seen 6 to 48 hrs after ischemia. At later time points (24-48 hrs), chromatin fragmentation was obvious in some cells (arrow in C and D). Representative of 8 experiments. **E**. TTC staining shows an infarct area of the barrel cortex 12 hrs after ischemia in the right hemisphere of the rat brain (see Figure 8A for TTC staining of ischemic infarct 24 hrs after ischemia in coronal brain sections).

Figure 2. Focal ischemic induced cell shrinkage in the ischemic region

Cell surface area was measured 16 hrs after ischemic insult using the ANALYSIS imaging software. A marked decrease in the cell surface area, likely represented by a cell volume decrease, was seen in the ischemic cortex compared with that in the same region of the contralateral side. Cell assay was performed under 40x magnification in 4 non-overlapping fields. N = 10 animals (3 brain sections per animal); *. $P < 0.05$ compared with no ischemia control by Student's t test and by Rank Sum Tests.

Figure 3. DNA damage of TUNEL positive cells after ischemia in the neonatal cortex

A. TUNEL positive cells (green) in the ischemic region 16 hrs after ischemia. Some cells show characteristics of DNA fragmentation (arrows), which are typical for the Type II TUNEL positive cells of apoptotic damage. Blue color is Hoechst staining of all

cells. **B**. Cell death in ischemic cortex was detected by TUNEL staining 1 hr to 14 days after ischemia. Cell death increased about 4 hrs after ischemia and reached a peak level around 16 to 48 hrs after ischemia. N = 8 - 10 animals for each time point (3 brain sections per animal).

Figure 4. Caspase activation after ischemic insult

A. Caspase-3 activation was detected using the CM-1 antibody. Noticeable CM-1 positive cells (dark brown) were seen in the ischemic region 12 hrs after ischemia. **B.** An enlarged image from the ischemic area in A. **C**. Time course of caspase-3 activity measured by DEVD cleavage. Significant caspase activation started from 4 hrs after ischemia and reached a peak level 8 to 24 hrs after ischemia. The gradual reduction in caspase activation was likely a combination of reduced enzyme activity and cell death. N = 8 - 10 animals for each time point (3 brain sections per animals). *. $P < 0.05$ compared with sham control.

Figure 5. Ischemia-induced cytochrome c release

Cytochrome c release into the cytoplasm was confirmed by immunostaining using the cytochrome c antibody (brown). **A**. Control staining of the contralateral brain. **B**. Positive cytochrome c staining was seen 6-12 hrs after ischemia in the ischemic region (the image shown was taken 12 hrs after ischemia). **C**. An enlarged image from the frame in B, showing the cytochrome c staining in cells. **D**. An enlarged image from the frame in C, showing the distribution of cytochrome c staining in the cytoplasm. Representative of 8 assays.

Figure 6. Ischemia-induced DNA damage induced neonatal brain

DNA was extracted from contralateral and ipsilateral sides of brains that underwent 4-, 6-, or 16-hr MCA occlusion. The extracted DNA was separated by agarose gel electrophoresis to detect DNA breaks. During the early time point of 4 hrs after ischemia, DNA smear breaks were prominent. The laddering pattern of DNA apoptotic damage was detected at 8 and 16 hrs after ischemia. N = 3.

Figure 7. Ultrastructural changes in damaged neurons in the ischemic cortex

Electron microscopy showed cellular and subcellular alterations of damaged neurons in ischemic region. **A**. A normal cortical neuron. **B**. Severely shrunken neurons 8 hrs after ischemia. Dark nuclei and condensed and fragmented chromatin (arrow) are evident in many cells. Meanwhile, some membrane and cytosolic disruption was also obvious in these cells. **C** and **D**. Ultrastructural changes 16 hrs after ischemia. Damaged cells show smaller cell bodies, apoptotic nuclear and chromatin condensation, and fragmentation (arrow). Formation of apoptotic bodies (arrow head) was seen in some cells such as the example in D. The necrotic alterations, however, took place in the cell cytoplasm, indicated by presence of large vacuoles (*), disappearance of cell organelles, and collapsed membranes. **E** and **F**. Neuronal damage 24 hrs after ischemia. The apoptotic nuclear changes (arrow) and formations of apoptotic bodies (arrow head) continued and the classical apoptotic “half-moon” nuclear morphology (unfilled arrow) was seen in some cells. Meanwhile, even more advanced necrotic deterioration developed in the cytoplasm and the cell membrane. N = 6.

Figure 8. Neuroprotective effect of EPO treatment in neonatal ischemic stroke

EPO was administrated 5-10 min before MCA occlusion (10,000 U/kg, i.p.) and followed by once per day until the day of sacrifice. **A**. Cerebral infarction in brain sections 24 hrs after whisker-barrel cortex ischemia, stained with TTC. Infarction and cavitation were reduced by EPO. **B**. Caspase/NeuN and TUNEL/Hoechst double staining in ischemic brain sections from control rats and in similar brain sections from rats that received EPO. Activated caspase-3 was stained by the anti-caspase 3 polyclonal antibody (green), assayed 16 hrs after ischemia. The red color shows NeuN staining of neuronal cells. TUNEL-staining (green) showed cell death in ischemic brain section from control and EPO-treated rats, 24 hrs after ischemia. Hoechst counterstaining (blue) showed all cells. **C**. Caspase activation measured by the anti-caspase-3 polyclonal antibody, summarized from experiments in B. EPO reduced caspase-3 activation in the ischemic region. N = 5. **D**. Summary of TUNEL positive cells in the ischemic region 24 hrs after ischemia. EPO treatment reduced the percentage of TUNEL positive cells. N = 5. **E**. EPO treatment markedly attenuated the ischemia-induced infarct volume 3 days after ischemia. N = 13 and 14 for ischemic control and EPO treated group, respectively. **F**. Stereotaxic measurements of infarct area at different coronal levels of the ischemic cortex, showing that EPO reduced infarct areas in sequential brain sections. N = 13 and 14 for ischemic control and EPO treated group, respectively. *. $P < 0.05$ compared with ischemic controls in C to F.

Figure 9. EPO increased STAT-5 and Bcl-2 levels in the ischemic brain

Western blot analysis of the ipsilateral cortex (ischemic and penumbra regions) different times after the focal ischemia. **A**. EPO administration (10,000 U/kg, i.p. 10-min before ischemia) increased phosphorylated STAT-5 level 12 and 24 hrs after ischemia compared with that without EPO. **B**. EPO also increased the anti-apoptotic gene Bcl-2 in the ipsilateral cortex. **C**. Quantitative summary of the EPO effects on STAT-5 and Bcl-2 immunoreactive bands 12 hrs after ischemia. The band intensity was corrected according to the protein loading of β-actin controls and expressed as percentage of the ischemic control levels. N = 3; *. $P < 0.05$ compared with stroke-only controls.

JPET Fast Forward. Published on December 15, 2005 as DOI: 10.1124/jpet.105.094391
This article has not been copyedited and formatted. The final version may differ from this version.

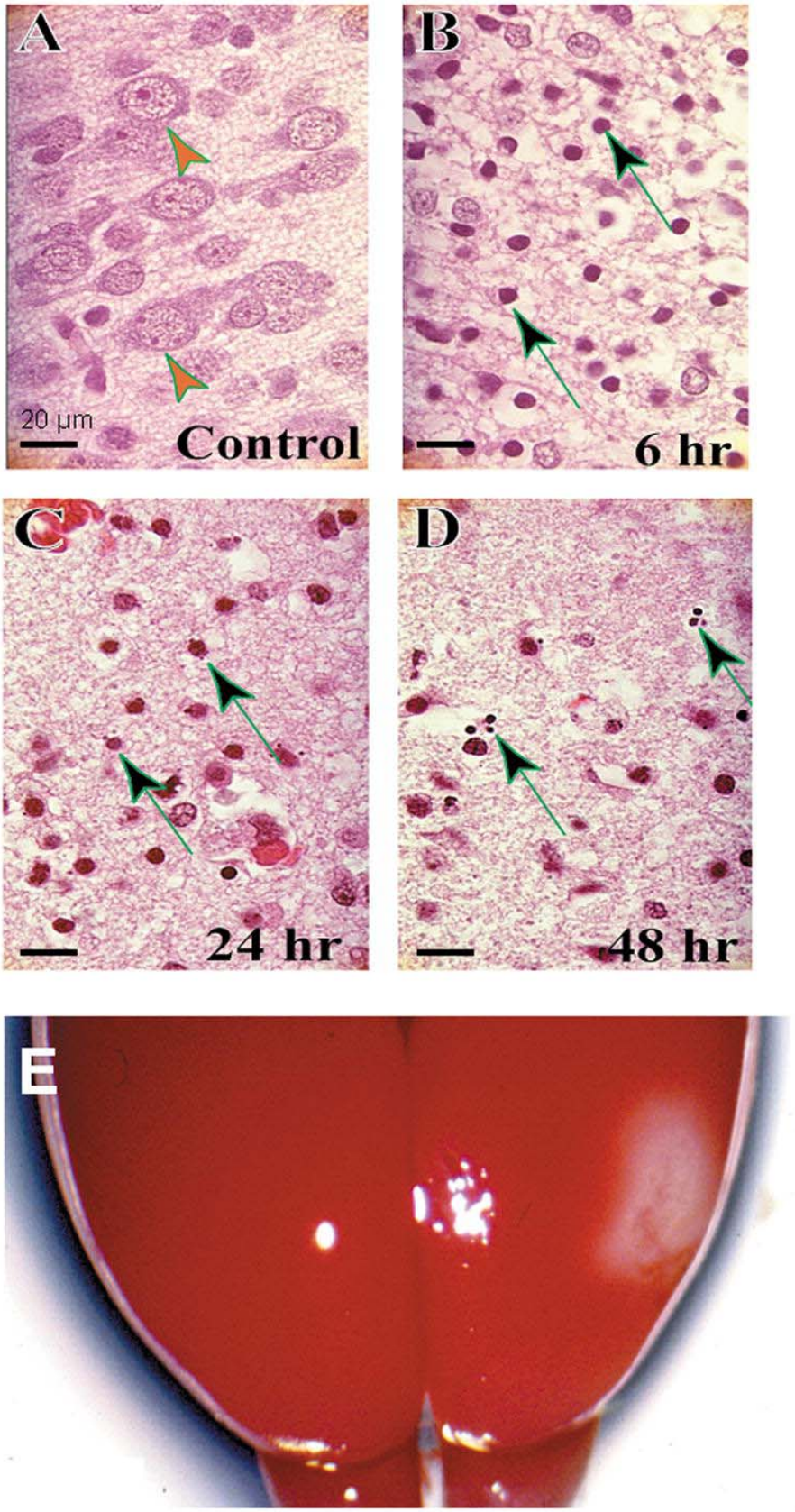

JPET Fast Forward. Published on December 15, 2005 as DOI: 10.1124/jpet.105.094391

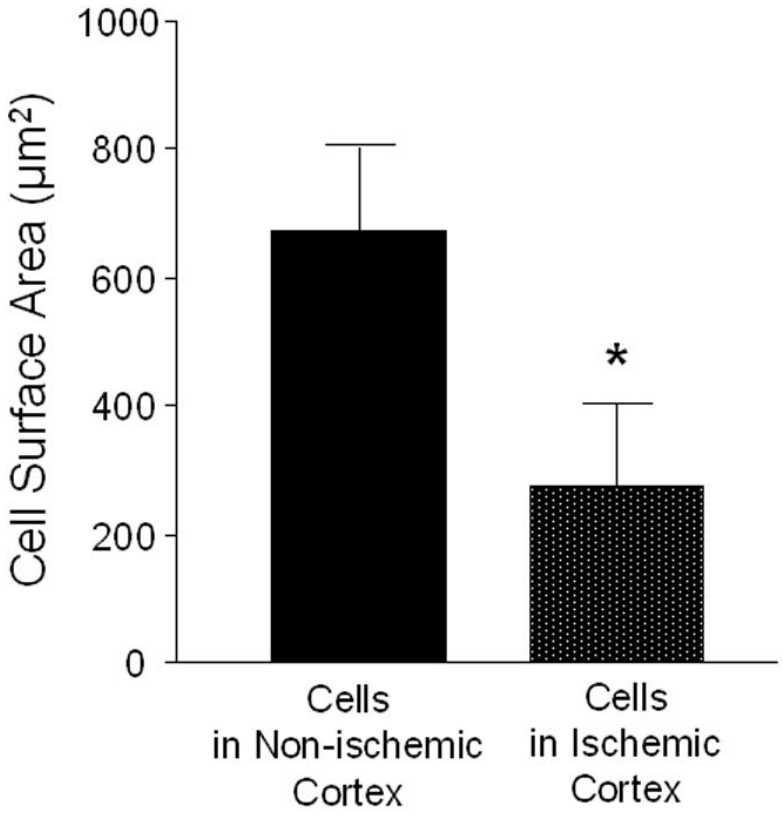

JPET Fast Forward. Published on December 15, 2005 as DOI: 10.1124/jpet.105.094391

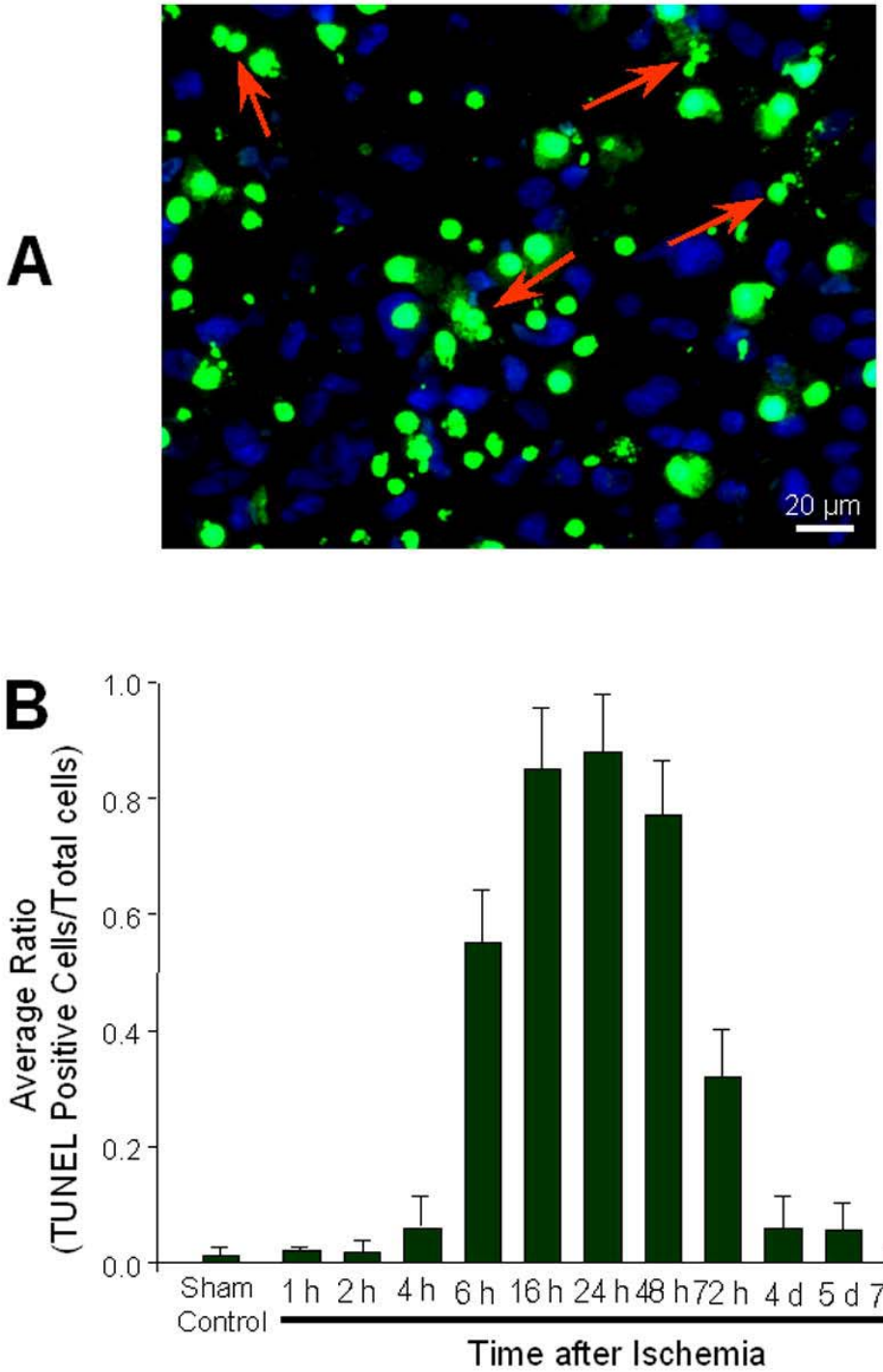

JPET Fast Forward. Published on December 15, 2005 as DOI: 10.1124/jpet.105.094391
This article has not been copyedited and formatted. The final version may differ from this version.

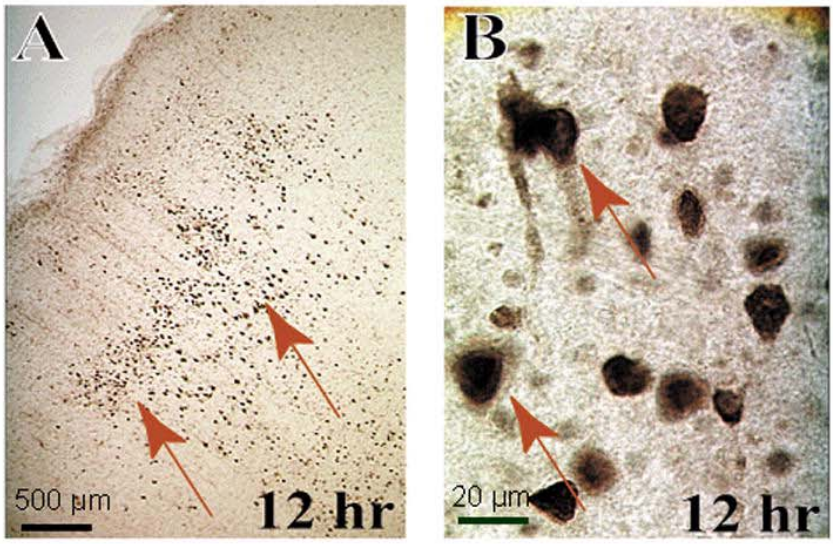

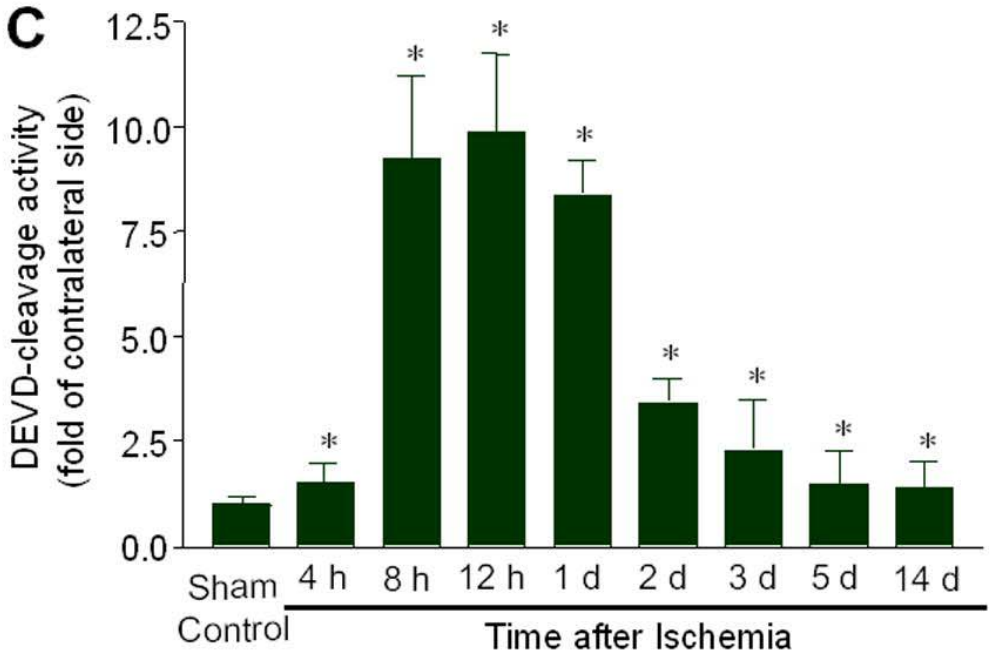

JPET Fast Forward. Published on December 15, 2005 as DOI: 10.1124/jpet.105.094391
This article has not been copyedited and formatted. The final version may differ from this version.

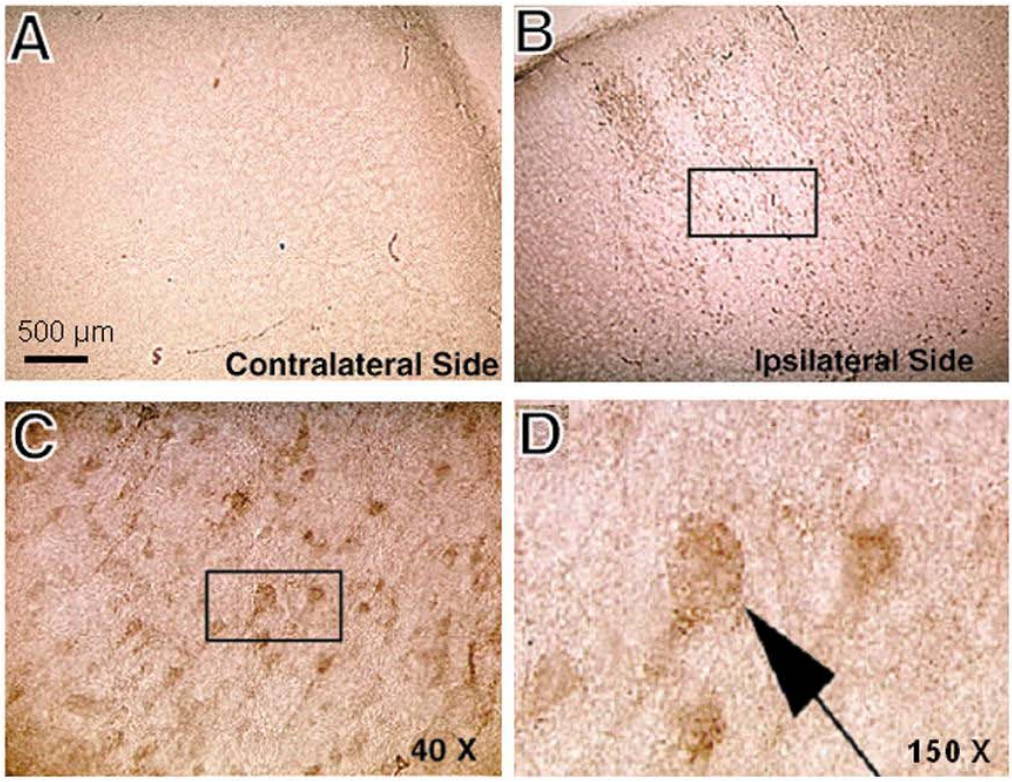

JPET Fast Forward. Published on December 15, 2005 as DOI: 10.1124/jpet.105.094391

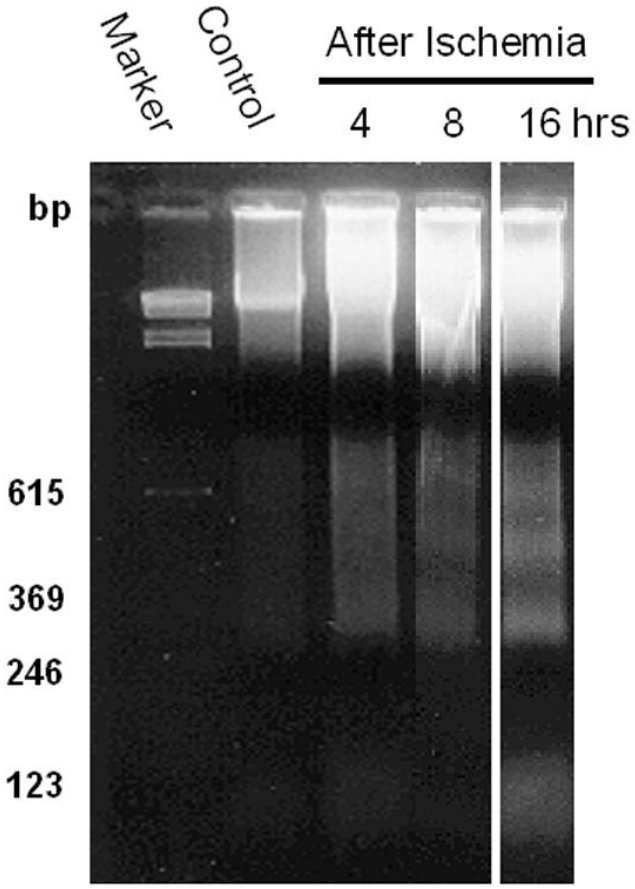

JPET Fast Forward. Published on December 15, 2005 as DOI: 10.1124/jpet.105.094391
This article has not been copyedited and formatted. The final version may differ from this version.

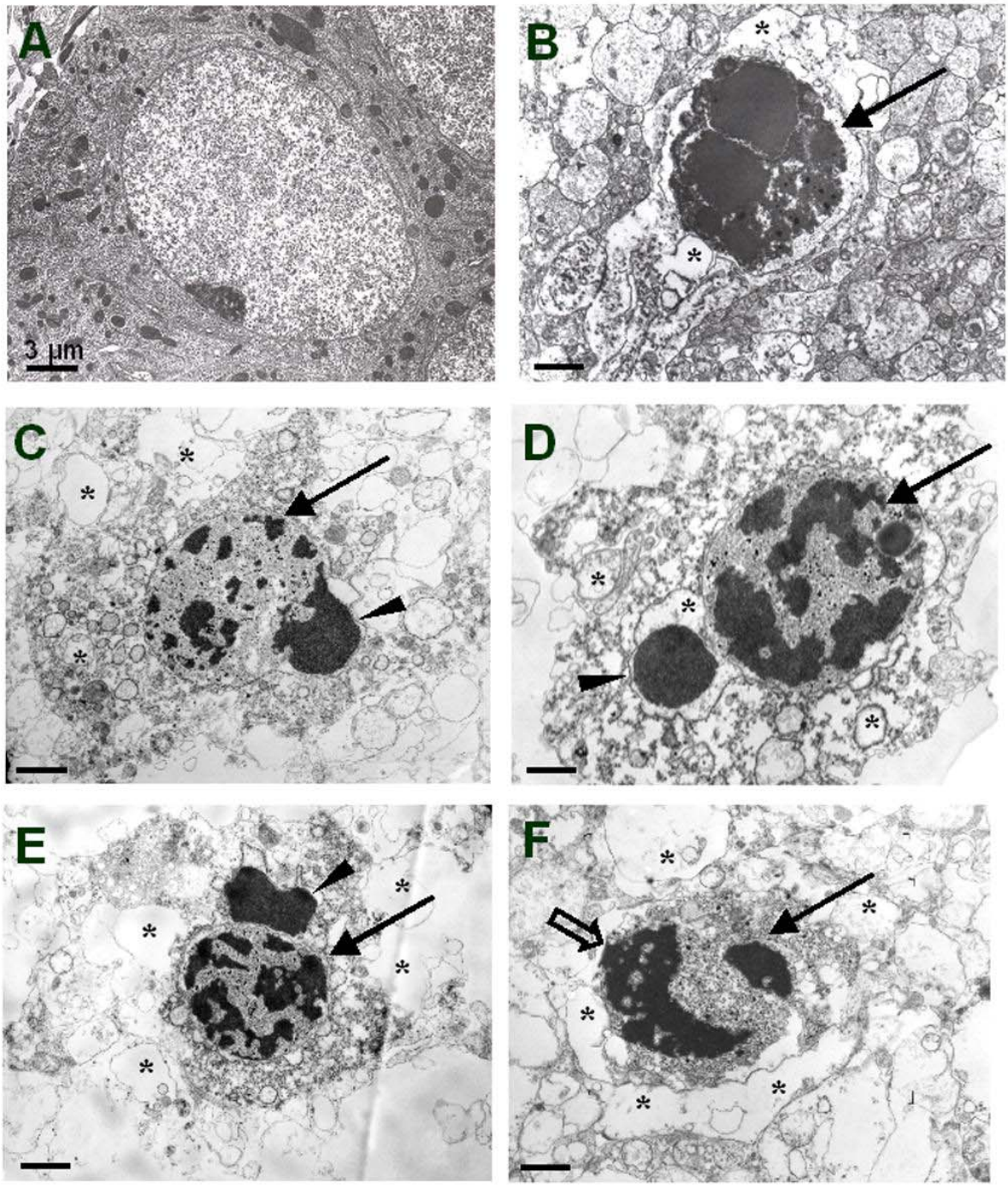

JPET Fast Forward. Published on December 15, 2005 as DOI: 10.1124/jpet.105.094391
This article has not been copyedited and formatted. The final version may differ from this version.

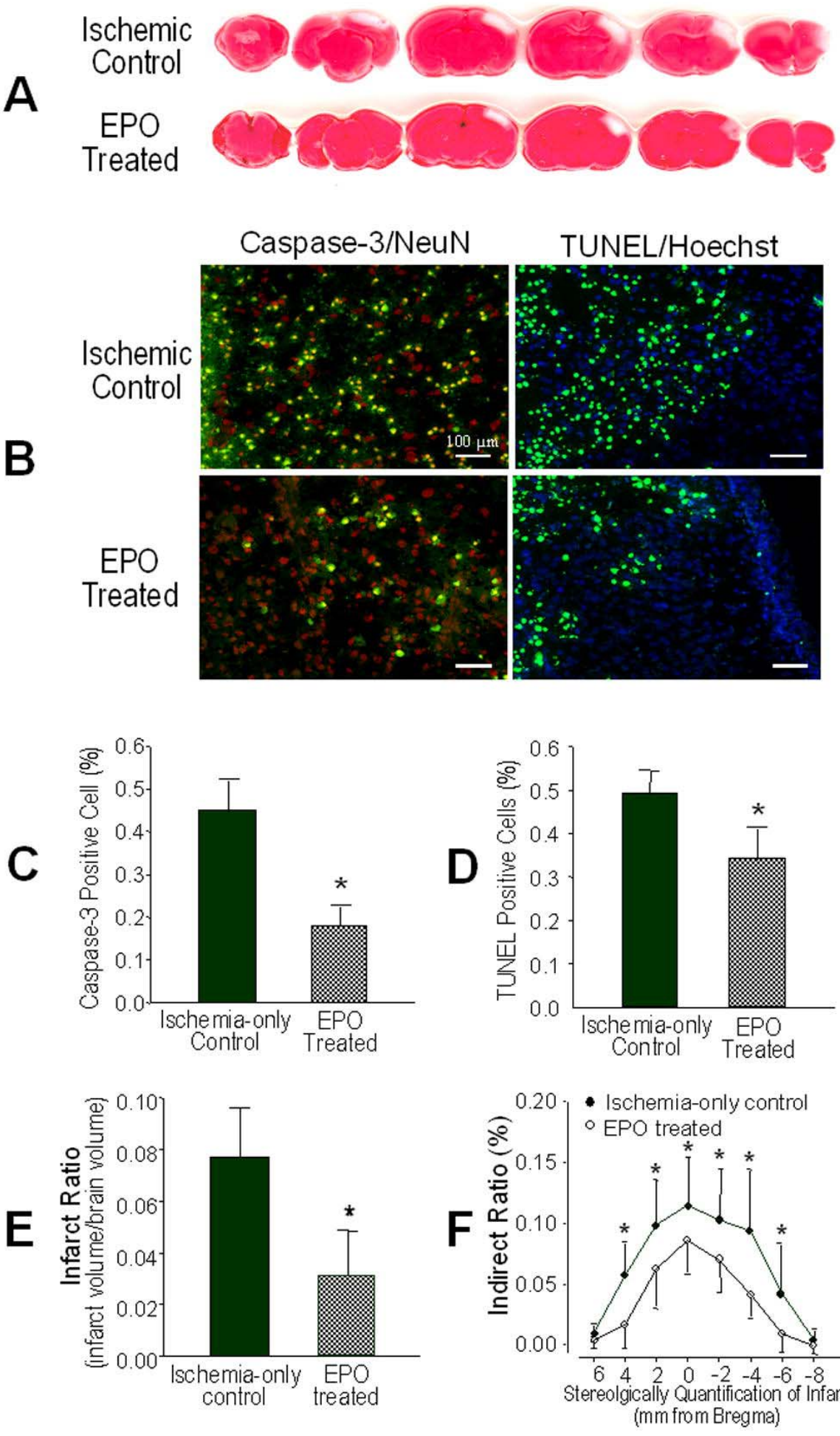

JPET Fast Forward. Published on December 15, 2005 as DOI: 10.1124/jpet.105.094391